Equilibrative Nucleoside Transporters: Mapping Regions of Interaction for the Substrate Analogue Nitrobenzylthioinosine (NBMPR) Using Rat Chimeric Proteins†

Manickavasagam Sundaram,‡ Sylvia Y. M. Yao,‡ Amy M. L. Ng,‡ Carol E. Cass,§ Stephen A. Baldwin,‖ and James D. Young*,‡

Membrane Transport Research Group, Departments of Physiology and Oncology, University of Alberta, and Cross Cancer Institute, Edmonton, Alberta T6G 2H7, Canada, and School of Biochemistry and Molecular Biology, University of Leeds, Leeds LS2 9JT, U.K.

Received January 29, 2001; Revised Manuscript Received April 25, 2001

ABSTRACT: The rat equilibrative nucleoside transporters rENT1 and rENT2 belong to a family of integral membrane proteins with 11 potential transmembrane segments (TMs) and are distinguished functionally by differences in sensitivity to inhibition by nitrobenzylthioinosine (NBMPR). Structurally, the proteins have a large glycosylated extracellular loop between TMs 1 and 2 and a large cytoplasmic loop between TMs 6 and 7. In the present study, we have generated chimeras between NBMPR-sensitive rENT1 and NBMPR-insensitive rENT2, using splice sites at rENT1 residues 99 (end of TM 2), 171 (between TMs 4 and 5), and 231 (end of TM 6) to identify structural domains of rENT1 responsible for transport inhibition by NBMPR. Transplanting the amino-terminal half of rENT2 into rENT1 rendered rENT1 NBMPR-insensitive. Domain swaps within the amino-terminal halves of rENT1 and rENT2 identified two contiguous regions, TMs 3−4 (rENT1 residues 100−171) and TMs 5−6 (rENT1 residues 172−231), as the major sites of NBMPR interaction. Since NBMPR is a nucleoside analogue and functions as a competitive inhibitor of zero-trans nucleoside influx, TMs 3−6 are likely to form parts of the substrate translocation channel.

Nucleosides participate in important biological processes (*1*−*4*). Tissues such as bone marrow and intestinal epithelial cells (and certain parasitic organisms), for example, lack de novo nucleotide synthetic pathways and rely on the salvage of exogenous nucleosides to maintain nucleotide pools (*3*, *4*). Synthetic analogues of physiological nucleosides are also widely used in cancer and viral chemotherapy (*5*−*7*). Since most nucleosides, including many nucleoside drugs, are relatively hydrophilic, specialized plasma membrane nucleoside transporter (NT)[1] proteins are required for their uptake or release from cells (*1*−*4*, *7*). Therefore, NT-mediated transport is a critical first step in nucleoside metabolism and in the pharmacological actions of anti-cancer and anti-viral nucleoside drugs. NTs also play a key role in regulating the extracellular concentration of adenosine in the vicinity of its cell surface receptors and thus influence processes such as neurotransmission and cardiovascular activity (*8*, *9*). Adenosine itself is used clinically to treat cardiac arrhythmias, and nucleoside transport inhibitors such as dipyridamole, dilazep, and draflazine function as coronary vasodilators (*1*−*3*).

Based on protein sequence homology and the underlying mechanism of transport, NTs can be classified into two major families (*10*−*20*). The concentrative nucleoside transporter proteins (designated as CNTs) mediate uphill nucleoside transport in a Na^+-dependent manner, whereas the equilibrative nucleoside transporter proteins (abbreviated as ENTs) function in a Na^+-independent manner and facilitate passive downhill transport. ENTs are more widely distributed than CNTs and occur in most, possibly all, cell types.

The equilibrative nucleoside transporters accept both pyrimidine and purine nucleosides as permeants and are subdivided into two types on the basis of their sensitivity to inhibition by nitrobenzylthioinosine (NBMPR) (*1*−*4*). Transporters of the equilibrative sensitive (*es*) type are potently inhibited by NBMPR (K_d = 0.1−10 nM). By contrast, transporters of the equilibrative insensitive (*ei*) type are little affected by concentrations of NBMPR in the micromolar range. cDNAs from human (h) and rat (r) tissues encoding proteins of both the *es* and *ei* subclasses have been cloned and are designated, respectively, h/rENT1 and h/rENT2, hENT2 and rENT2 being NBMPR-insensitive (*17*−*20*). They also differ in sensitivity to inhibition by vasodilators (hENT1 > hENT2 > rENT1 = rENT2) (*17*−*20*), and by the ability of hENT2 and rENT2 to transport nucleobases as well as nucleosides (*2*, *4*, *20*, *21*). Structurally, the 4 proteins are predicted to have a common membrane topology of 11

† This work was supported in part by the Canadian Institutes of Health Research, the Wellcome Trust, and the Medical Research Council of the United Kingdom. J.D.Y. is a Heritage Scientist of the Alberta Heritage Foundation for Medical Research (AHFMR). M.S. was funded by an AHFMR Postdoctoral Fellowship.

* To whom correspondence should be addressed. Tel: 780-492-5895. Fax: 780-492-7566. E-mail: james.young@ualberta.ca.

‡ Department of Physiology, University of Alberta.

§ Department of Oncology, University of Alberta, and Cross Cancer Institute.

‖ University of Leeds.

[1] Abbreviations: CNT, concentrative nucleoside transporter; ENT, equilibrative nucleoside transporter; NBMPR, nitrobenzylthioinosine (6-[(4-nitrobenzyl)thio]-9-β-D-ribofuranosylpurine); NT, nucleoside transporter; PCMBS, *p*-chloromercuriphenyl sulfonate; TM, putative transmembrane helix.

10.1021/bi0101805 CCC: $20.00
Published on Web 06/13/2001

transmembrane segments (TMs), with a large glycosylated extracellular loop between TMs 1 and 2 and a large cytoplasmic loop between TMs 6 and 7. Sequence homology between family members is greatest within putative TM regions.

In a previous paper (*22*), we used the difference in vasodilator sensitivity between hENT1 (vasodilator-sensitive) and rENT1 (vasodilator-resistant) as the rationale to construct chimeras between the two proteins to identify transporter regions responsible for vasoactive drug binding. It was established that vasoactive drug inhibition involved two domains in the amino-terminal half of hENT1 (TMs 1−2 and TMs 3−6), with TMs 3−6 being the major site of interaction. Functional studies suggest that vasodilators and NBMPR compete with permeant for binding to common or overlapping exofacial sites within the substrate translocation channel of the transporter (*2*, *23*−*26*). However, the general structures of vasoactive compounds are significantly different from the nucleoside derivative NBMPR, and they inhibit nucleoside transport with lower apparent affinities than NBMPR [dipyridamole K_i = 200 nM for recombinant hENT1 (*22*)]. More significantly, a number of studies have reported that dipyridamole inhibits dissociation of bound NBMPR, a finding inconsistent with simple single-site models of ligand binding (reviewed in ref *2*). We therefore decided to employ a similar chimeric strategy to our vasodilator study (*22*) to investigate transporter interactions with NBMPR.

To determine NBMPR binding domains free from any structural elements involved in vasodilator interactions, the rat transporters rENT1 and rENT2 were employed, both of which are resistant to inhibition by vasoactive drugs (*18*). Taking advantage of the marked difference in NBMPR sensitivity between the two transporters (*18*), a series of rENT1/rENT2 chimeric molecules were generated to identify regions of rENT1 responsible for NBMPR recognition. Since NBMPR and its congeners are derivatives of physiological nucleosides and share with them common structural requirements for optimal activity (*2*), it was anticipated that these chimeras would provide definitive information on the location of the substrate translocation channel of the transporter. The chimeric proteins were expressed in *Xenopus* oocytes and evaluated for transport function and sensitivity to NBMPR inhibition. Our results suggest that the structural determinants for NBMPR binding are located within putative TMs 3−6, with TMs 3−4 and 5−6 contributing almost equally to binding affinity. TMs 1−2 did not appear to play any role in NBMPR inhibition, which is different from the situation seen with vasoactive compounds (*22*).

EXPERIMENTAL PROCEDURES

Construction of Chimeras. cDNAs encoding rENT1 and rENT2 (Figure 1) were cloned into the vector pGEM-T (Promega) as previously described (*18*). An overlap extension PCR method (*27*) was used to amplify and link appropriate segments of cDNAs. Chimeric cDNAs generated by *Pyrococcus furiosus* DNA polymerase were then subcloned into *Sal*I and *Sph*I sites of pGEM-T. All constructs were fully sequenced in both directions to confirm that the desired chimeras were obtained and that no point mutations had been introduced by PCR. The nomenclature and composition of the chimeras are shown in Figure 2. Those constructed by sequential transplantation of fragments of rENT2 into rENT1 (the rENT1 series) are designated by the letter R, with the numbers in parentheses indicating putative TM segments of rENT2 (including the loops) transplanted into equivalent positions of rENT1 (Figure 2A). For instance, R(1−6) is a 50:50 chimeric transporter whose TMs 1−6 (amino-terminal half) are from rENT2 and whose central cytoplasmic loop plus TMs 7−11 (carboxyl-terminal half) are from rENT1; R(1−2) is a 25:75 chimeric transporter whose TMs 1−2 (amino-terminal one-fourth) are from rENT2 and whose TMs 3−11 (carboxyl-terminal three-fourths) are from rENT1; R(3−4) is a chimeric transporter with TMs 3−4 from rENT2 and the rest of the protein from rENT1. Similarly, r(3−6) designates a reciprocal rENT2 series chimera in which TMs 3−6 of rENT1 were introduced into rENT2 (Figure 2B). The three junction points used to construct the chimeras are represented by arrows A, B, and C in Figure 1.

In Vitro Transcription and Expression in Xenopus Oocytes. pGEM-T containing rENT1, rENT2, and chimeras R(1−6), R(1−2), R(3−6), R(3−4), R(5−6), and r(3−6) was linearized with *Sph*I and transcribed with SP6 polymerase using the mMESSAGE mMACHINE (Ambion) transcription system. Defolliculated stage VI *Xenopus* oocytes (*18*) were injected with 20 nL of water or with 20 nL of water containing capped RNA transcript (20 ng) and incubated in modified Barth's medium (changed daily) at 18 °C for 72 h prior to the assay of transport activity.

Transport Assays. Transport experiments were performed as described previously (*17*, *18*) on groups of 12 oocytes at 20 °C using [^{14}C]uridine (Amersham Pharmacia Biotech) (1 μCi/mL) in 200 μL of transport buffer containing 100 mM NaCl, 2 mM KCl, 1 mM $CaCl_2$, 1 mM $MgCl_2$, and 10 mM HEPES, pH 7.5. Initial rates of uridine uptake (10 μM) were determined using an incubation period of 2 min for rENT1, rENT2, and R(1−2), or 30 min for R(1−6), R(3−6), R(3−4), R(5−6), and r(3−6). To ensure maximum inhibition, oocytes were pretreated with NBMPR (1 μM unless otherwise stated) for 1 h before the addition of permeant (*17*, *18*). The influx values shown are corrected for endogenous nucleoside uptake (measured in control water-injected cells) and represent the means ± SE of 10−12 oocytes. Each experiment was performed at least twice on different batches of oocytes.

RESULTS AND DISCUSSION

Wild-Type rENT1 and rENT2. The amino acid sequences of rENT1 (457 residues) (*18*) and rENT2 (456 residues) (*18*) are 50% identical and 69% similar. Hydropathy analyses suggest a common membrane architecture with 11 potential TMs. As shown in Figure 1, residues conserved between the two proteins, which may have structural/functional significance, are located largely within the putative TMs. The putative *N*-linked glycosylation site at Asn^{48} of rENT1 is conserved in both hENT1 (Asn^{48}) and rENT2 (Asn^{47}). We have used site-directed mutagenesis to confirm the identity of Asn^{48} as the only site of glycosylation in hENT1 (*28*), and it is likely that the same also applies to rENT1. When expressed in *Xenopus* oocytes, rENT1 and rENT2 mediate saturable uridine influx (apparent K_m values of 0.15 and 0.30 mM, respectively), are broadly selective for purine and

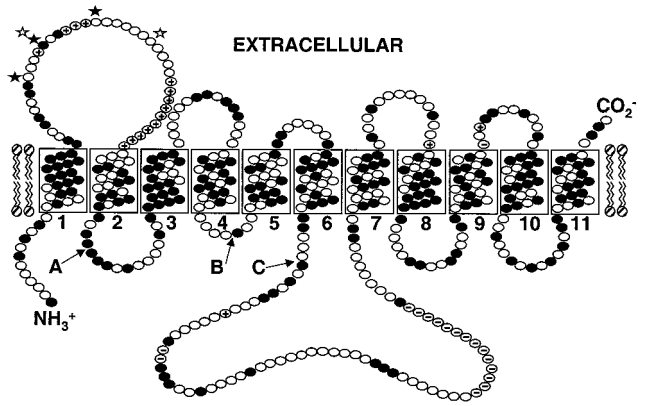

FIGURE 1: Topographical model of rENT1 and rENT2. Hydropathy profiles for the predicted amino acid sequences of rENT1 and rENT2 were determined by the method of Eisenberg et al. (*31*). Potential membrane-spanning α-helices in the topographical model are numbered, and putative glycosylation sites in rENT1 and rENT2 are indicated by solid and open stars, respectively. Residues identical in the two proteins are shown as darkened circles. Residues corresponding to insertions in the sequences of rENT1 or rENT2 are indicated by circles containing "+" and "−" signs, respectively. Splice sites used for the construction of chimeras are represented by arrows A, B, and C.

pyrimidine nucleosides, including adenosine, and are insensitive to inhibition by dipyridamole, dilazep, or draflazine (*18*). Despite these similarities, the two transporters differ markedly (2−3 orders of magnitude) in their sensitivity to inhibition by NBMPR (*18*). rENT2, but not rENT1, transports nucleobases in addition to nucleosides (*4*). We have exploited the difference in NBMPR sensitivity to identify regions of rENT1 responsible for NBMPR binding.

Construction of Chimeras. The nomenclature and composition of the chimeras are shown in Figure 2. Five chimeras (the rENT1 series) were constructed by introducing regions of rENT2 into homologous regions of rENT1 (Figure 2A). Using the topology model shown in Figure 1, splice sites were engineered within cytoplasmic domains adjacent to residues conserved in the two proteins, thereby minimizing disruption to native TMs and loops. Graft site A was close to the start of the first putative cytoplasmic loop between residues 99 and 100 of rENT1. Graft site B was about the middle of the second cytoplasmic loop between residues 171 and 172 of rENT1. Graft site C was close to the start of the large central cytoplasmic loop between residues 231 and 232. Graft sites A and C were in positions corresponding to those used previously to generate chimeras between hENT1 and rENT1 (*22*), and were also used to construct a reciprocal rENT2 series chimera in which residues 100−231 of rENT1 were inserted into the homologous region of rENT2 (Figure 2B).

Functional Production of Parental and rENT1 Series Chimeric Transporters. RNA transcripts for rENT1, rENT2, and each of the rENT1 series of chimeras were expressed in *Xenopus* oocytes and assayed for nucleoside transport activity (10 μM uridine influx) in the absence or presence of NBMPR as described under Experimental Procedures (*17*, *18*). Endogenous nucleoside uptake was measured in water-injected oocytes. Each of the five chimeras R(1−2), R(1−6), R(3−6), R(3−4), and R(5−6) transported uridine, suggesting that the native conformation was generally retained in all constructs. R(1−6), R(3−6), R(3−4), and R(5−6) displayed

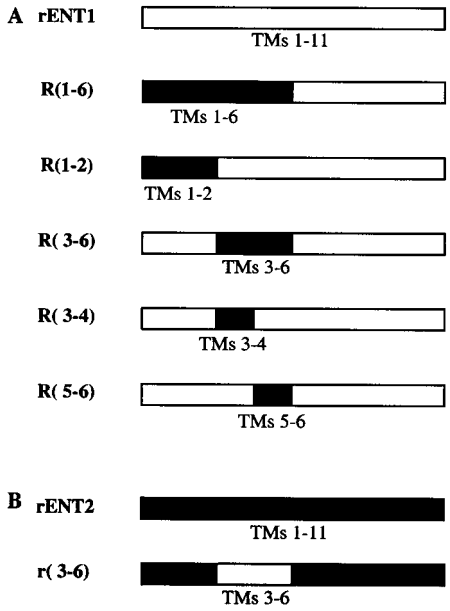

FIGURE 2: Schematic representation of rENT1/rENT2 chimeric constructs. Shown is a diagrammatic representation of the junction points of the chimeric species used in this study. These correspond to the start of the first cytoplasmic loop, the middle of the second cytoplasmic loop, and the start of the third cytoplasmic loop. Regions derived from rENT2 are shown as black bars, and those from rENT1 are shown as white bars. The nomenclature used in this study is indicated. For the five rENT1 series chimeras (designated by the letter R), numbers in parentheses refer to putative TM segments of rENT2 that were transplanted into equivalent positions of rENT1 (A). For the reciprocal rENT2 series chimera (designated by the letter r), numbers in parentheses refer to putative TM segments of rENT1 that were transplanted into equivalent positions of rENT2 (B).

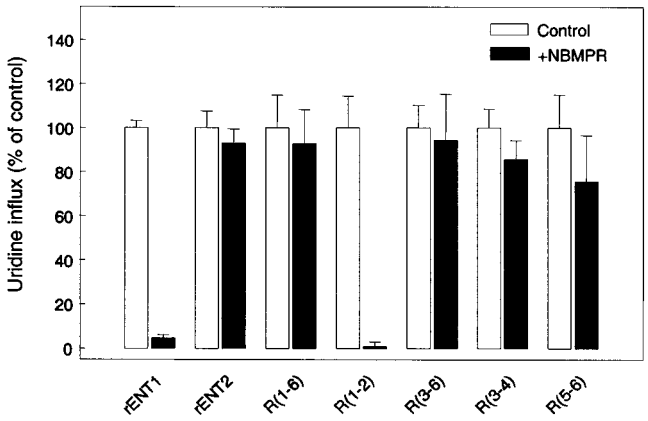

FIGURE 3: Inhibition of rENT1, rENT2, and rENT1 series chimeras by 1 μM NBMPR. Initial rates of uridine uptake were measured in the absence (white bars) and in the presence of NBMPR (black bars) in oocytes injected with 20 ng of RNA transcript encoding wild-type rENT1 or rENT2 or one of the chimeric transporters. Results are corrected for endogenous nucleoside transport activity (measured in water-injected oocytes) and expressed as a percentage of the uninhibited flux for each transporter. Values are means ± SE for 10−12 oocytes.

lower levels of functional expression than R(1−2), rENT1, or rENT2 and required a longer incubation period (30 min versus 2 min) to obtain comparable levels of total uptake. One reason for this could be reduced plasma membrane targeting. Nevertheless, all constructs gave fluxes large enough to determine their sensitivity to inhibition by NBMPR. Influx values, corrected for endogenous uptake in

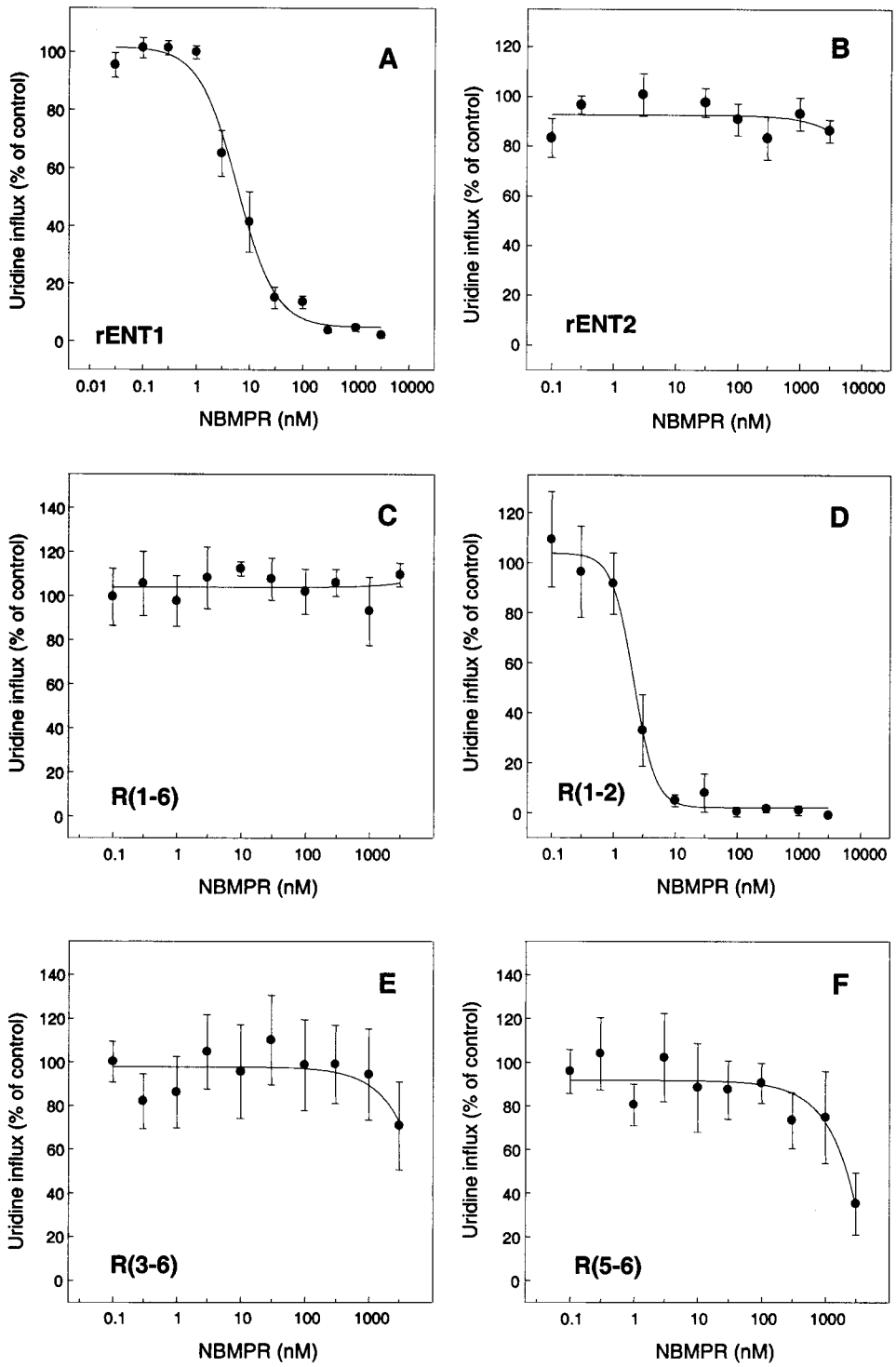

FIGURE 4: Dose−response curves for NBMPR inhibition of rENT1, rENT2, and rENT1 series chimeras. Initial rates of uridine uptake in the presence of increasing concentrations of NBMPR (0.3 nM−3 μM) were corrected for endogenous nucleoside transport activity (measured in water-injected oocytes) and expressed as a percentage of the uninhibited flux for each transporter: rENT1 (A), rENT2 (B), R(1−6) (C), R(1−2) (D), R(3−6) (E), and R(5−6) (F). Values are means ± SE for 10−12 oocytes.

water-injected oocytes, were in the range 1.7−2.2 pmol/oocyte·2 min^{-1} for rENT1, rENT2, and R(1−2), and 1.3−4.4 pmol/oocyte·30 min^{-1} for the other chimeras, R(3−4) consistently showing the lowest activity. The corresponding endogenous uridine influx values in water-injected oocytes were 0.010−0.014 pmol/oocyte·2 min^{-1} and 0.13−0.32 pmol/oocyte·30 min^{-1}, respectively.

NBMPR Inhibition of Parental and rENT1 Series Chimeric Transporters. The effects of NBMPR on the rENT1 series of chimeric transporters were investigated, in the first instance, at a single concentration of 1 μM. As illustrated in the representative experiment shown in Figure 3, this concentration of NBMPR caused almost complete inhibition of rENT1 but had no effect on rENT2 (see also ref *18*). The first chimera of the series, R(1−6), was a 50:50 construct in which TMs 1−6 of rENT1 (representing the amino-terminal half of rENT1) were replaced by those of rENT2 (the splice site is shown as arrow C in Figure 1). NBMPR was unable

to inhibit uridine transport mediated by this chimera, suggesting that the site(s) of NBMPR interaction lie(s) within the amino-terminal half of rENT1.

To identify the NBMPR recognition domains within the amino-terminal half of rENT1, a splice site was designed near the middle of TMs 1−6 (arrow A in Figure 1), thereby producing two chimeric transporters, R(1−2) and R(3−6). The construct R(1−2), composed of rENT2 from the amino terminus to the end of TM 2 and rENT1 for the rest of the protein, was NBMPR-sensitive, and the extent of inhibition was very similar to that of wild-type rENT1 (Figure 3). The absence of a decrease in NBMPR inhibition when TMs 1−2 of rENT1 were substituted with TMs 1−2 of rENT2 suggested that this part of rENT1 was not involved in determining NBMPR sensitivity. Thus, chimera R(1−2) narrowed the region of interest to TMs 3−6 and the 12 residues of the preceding intracellular loop. For simplicity, we will hereafter refer to this region as TMs 3−6, and the abbreviation TMs 1−2 will be used to describe the domain from the amino terminus to the end of TM 2.

The next chimeric transporter in the series, R(3−6), was created by substituting TMs 3−6 of rENT1 with the corresponding region of rENT2. As predicted by the characteristics of R(1−6) and R(1−2), chimera R(3−6) was unaffected by 1 μM NBMPR. Thus, replacement of TMs 3−6 of rENT1 resulted in complete loss of NBMPR sensitivity, suggesting that the structural components responsible for interaction with NBMPR reside in this region.

To further localize NBMPR binding site(s) within TMs 3−6 of rENT1, microdomain swaps were carried out in this region (the splice site is shown as arrow B in Figure 1), giving rise to chimeras R(3−4) and R(5−6). When tested for inhibition by NBMPR, both chimeras were largely insensitive to NBMPR, suggesting that both TMs 3−4 and TMs 5−6 contributed to recognition of NBMPR.

To quantify the relative contributions of different transporter domains to NBMPR inhibition, full NBMPR dose−response curves (0.3 nM−3 μM inhibitor) were determined for rENT1, rENT2, and each of the chimeras [with the exception of low activity R(3−4)]. Representative results are shown in Figure 4. Chimera R(1−2) exhibited an IC_{50} value (±SE) similar to that of wild-type rENT1 (2.3 ± 1.9 and 4.2 ± 1.4 nM, respectively), while R(1−6) and R(3−6) resembled rENT2 and showed no significant inhibition by NBMPR at concentrations up to 3 μM. R(5−6) retained residual sensitivity to NBMPR inhibition (IC_{50} value of 3.7 ± 0.1 μM), consistent with the participation of both TMs 3−4 and TMs 5−6 in NBMPR binding.

Functional Production and NBMPR Inhibition of rENT2 Series Chimera r(3−6). Involvement of the TM 3−6 region in NBMPR inhibition was confirmed by constructing a reciprocal rENT2 series chimera in which TMs 3−6 of rENT2 were replaced by those of rENT1 (splice sites shown by arrows A and C in Figure 1). As illustrated in the representative experiment shown in Figure 5, r(3−6) was functional when produced in *Xenopus* oocytes and, as predicted from studies of the rENT1 series of chimeras, was NBMPR-sensitive (mediated uridine influx of 0.44 ± 0.05 pmol/oocyte•30 min^{-1} inhibited 82% by 1 μM NBMPR).

Concluding Remarks. The major protein sequence differences between rENT1 and rENT2 lie in the large extracellular loop between TMs 1 and 2 and in the putative central cytoplasmic loop between TMs 6 and 7. In addition, the extracellular loop of rENT2 between TMs 1 and 2 contains 14 fewer amino acids than rENT1, while its central cytoplasmic loop linking TMs 6 and 7 has 14 more residues than rENT1. It might be anticipated, therefore, that these loops could be involved in the different NBMPR sensitivities displayed by the two transporters. The present chimeric study has eliminated involvement of these regions and, as well, the carboxy-terminal half of the protein. Our results suggest instead that the structural requirements for NBMPR sensitivity reside within TMs 3−6 (residues 100−231 of rENT1), the same region previously implicated in vasodilator binding (*22*). The amino terminus up to the end of TM 2 (including the large extracellular loop) also contributes to vasodilator sensitivity (*22*), but, as shown here, plays no apparent role in the inhibitory action of NBMPR. Therefore, our results provide structural evidence that NBMPR and vasodilators occupy overlapping, but not identical, sites on equilibrative nucleoside transporters. This finding is consistent with a large body of previous kinetic and ligand binding studies of native *es*-type transporters, but is at odds with reports that dipyridamole inhibits dissociation of bound NBMPR (*2*). In their review of this topic, Griffith and Jarvis (*2*) propose that the latter effect results from binding of dipyridamole to a secondary low-affinity allosteric site on the transporter.

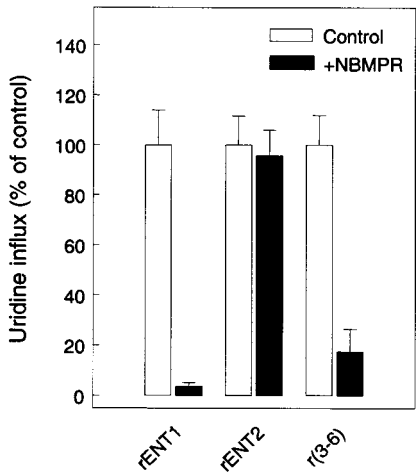

FIGURE 5: Inhibition of the rENT2 series chimera r(3−6) by 1 μM NBMPR. Initial rates of uridine uptake were measured in the absence (white bars) and in the presence of NBMPR (black bars) in oocytes injected with 20 ng of RNA transcript encoding wild-type rENT1 or rENT2 or the chimeric transporter r(3−6). Results are corrected for endogenous nucleoside transport activity (measured in water-injected oocytes) and expressed as a percentage of the uninhibited flux for each transporter. Values are means ± SE for 10−12 oocytes.

Since NBMPR is a nucleoside analogue and competes with permeant (and vasodilators) for binding to exofacial domains within the substrate translocation channel of the transporter, we deduce that elements of the TM 3−6 region contribute to the nucleoside permeation pathway of the transporter. In support of this conclusion, we have recently identified in rENT2 a unique cysteine residue (Cys^{140}) that is responsible for sensitivity to inhibition by extracellular PCMBS (*29*). This Cys residue is located in the outer half of putative TM4 (Figure 1) and is within the structural domain (TMs 3−6) identified here as responsible for interactions with NBMPR. PCMBS binding to rENT2 Cys^{140} was prevented by extracellular uridine, suggesting that this residue and the helix to

which it belongs (TM 4) lie within or are closely adjacent to the substrate translocation channel of the transporter. Our demonstration that NBMPR binding involves domains within TMs 5−6 as well as TMs 3−4 suggests that residues in TMs 5−6 also contribute to the substrate translocation channel. Within these four TMs, the amino acid sequences of rENT1 and rENT2 are 62% identical and 71% similar, with differences between the two proteins occurring mainly as single or double residue substitutions. Thus, our results provide a starting point for a detailed analysis of NBMPR binding by scanning mutagenesis of unconserved residues.

Finally, the present findings provide a structural basis to interpret previous NBMPR photoaffinity labeling studies of the purified human erythrocyte *es* (hENT1) nucleoside transporter (*30*). These experiments used enzymic cleavage to establish that the site of covalent attachment of NBMPR was within 16 kDa of the site of N-linked glycosylation (*30*), now identified as Asn^{48} in the loop between TMs 1 and 2 (*28*).

REFERENCES

1. Cass, C. E. (1995) in *Drug Transport in Antimicrobial and Anticancer Chemotherapy* (Georgopapadakou, N. H., Ed.) pp 404−451, Marcel Dekker, New York.
2. Griffith, D. A., and Jarvis, S. M. (1996) *Biochim. Biophys. Acta 1286*, 153−181.
3. Baldwin, S. A., Mackey, J. R., Cass, C. E., and Young, J. D. (1999) *Mol. Med. Today 5*, 216−224.
4. Young, J. D., Cheeseman, C. I., Mackey, J. R., Cass, C. E., and Baldwin, S. A. (2000) *Curr. Top. Membr. 50*, 329−378.
5. Periguad, C., Gosselin, G., and Imbach, J. L. (1992) *Nucleosides Nucleotides 11*, 903−945.
6. Handschumacher, R. E., and Cheng, C. Y. (1993) in *Cancer Metabolism* (Holland, E., Frei, E., Bast, R. C., Kufe, D. W., Morton, D. L., and Weichselbaum, R. R., Eds.) pp 712−732, Lea & Febiger, Philadelphia.
7. Mackey, J. R., Baldwin, S. A., Young, J. D., and Cass, C. E. (1998) *Drug Resist. Updates 1*, 310−324.
8. Fredholm, B. B. (1997) *Curr. Med. Chem. 4*, 35−66.
9. Shryock, J. C., and Belardinelli, L. (1997) *Am. J. Cardiol. 79*, 2−10.
10. Huang, Q. Q., Yao, S. Y. M., Ritzel, M. W. L., Paterson, A. R. P., Cass, C. E., and Young, J. D. (1994) *J. Biol. Chem. 269*, 17757−17760.
11. Che, M., Ortiz, D. F., and Arias, I. M. (1995) *J. Biol. Chem. 270*, 13596−13599.
12. Yao, S. Y. M., Ng, A. M. L., Ritzel, M. W. L., Gati, W. P., Cass, C. E., and Young, J. D. (1996) *Mol. Pharmacol. 50*, 1529−1535.
13. Ritzel, M. W. L., Yao, S. Y. M., Huang, M. Y., Elliot, J. F., Cass, C. E., and Young J. D. (1997) *Am. J. Physiol. 272*, C707−C714.
14. Wang, J., Su, S. F., Dresser, M. J., Schaner, M. E., Washington, C. B., and Giacomini, K. M. (1997) *Am J. Physiol. 273*, F1058−F1065.
15. Ritzel, M. W. L., Yao, S. Y. M., Ng, A. M. L., Mackey, J. R., Cass, C. E., and Young, J. D. (1998) *Mol. Membr. Biol. 15*, 203−211.
16. Ritzel, M. W. L., Ng, A. M. L., Yao, S. Y. M., Graham, K., Loewen, S. K., Smith, K. M., Ritzel, G., Mowles, D. A., Carpenter, P., Chen, X. Z., Karpinski, E., Hyde, R. J., Baldwin, S. A., Cass, C. E., and Young, J. D. (2001) *J. Biol. Chem. 276*, 2914−2927.
17. Griffiths, M., Beaumont, N., Yao, S. Y. M., Sundaram, M., Bouman, C. E., Davies, A., Kwong, F. Y. P., Coe, I. R., Cass, C. E., Young, J. D., and Baldwin, S. A. (1997) *Nat. Med. 3*, 89−93.
18. Yao, S. Y. M., Ng, A. M. L., Muzyka, W. R., Griffiths, M., Cass, C. E., Baldwin, S. A., and Young, J. D. (1997) *J. Biol. Chem. 272*, 28423−28430.
19. Griffiths, M., Yao, S. Y. M., Abidi, F., Phillips, S. E. V., Cass, C. E., Young, J. D., and Baldwin, S. A. (1997) *Biochem. J. 328*, 739−743.
20. Crawford, C. R., Patel, D. H., Naeve, C., and Belt, J. A. (1998) *J. Biol. Chem. 273*, 5288−5293.
21. Osses, N., Pearson, J. D., Yudilevich, D. L., and Jarvis, S. M. (1996) *Biochem. J. 317*, 843−848.
22. Sundaram, M., Yao, S. Y. M., Ng, A. M. L., Griffiths, M., Cass, C. E., Baldwin, S. A., and Young, J. D. (1998) *J. Biol. Chem. 267*, 21954−21960.
23. Jarvis, S. M., McBride, D., and Young, J. D. (1982) *J. Physiol. (London) 324*, 31−46.
24. Jarvis, S. M., Janmohamed, N. S., and Young, J. D. (1983) *Biochem. J. 216*, 661−667.
25. Jarvis, S. M. (1986) *Mol. Pharmacol. 30*, 658−665.
26. Agbanyo, F. R., Cass, C. E., and Paterson, A. R. P. (1988) *Mol. Pharmacol. 33*, 332−337.
27. Horton, R. M., Hunt, H. D., Ho, S. N., Pullen, J. K., and Pease, L. R. (1989) *Gene 77*, 61−68.
28. Vickers, M. F., Yao, S. Y. M., Baldwin, S. A., Young, J. D., and Cass, C. E. (2000) *J. Biol. Chem. 275*, 25931−25938.
29. Yao, S. Y. M., Sundaram, M., Chomey, E. G., Cass, C. E., Baldwin, S. A., and Young, J. D. (2001) *Biochem. J. 353*, 387−393.
30. Kwong, F. Y. P., Wu, J. S. R., Fincham, H. E., Davies, A., Henderson, P. J. F., Baldwin, S. A., and Young, J. D. (1993) *J. Biol. Chem. 268*, 22127−22134.
31. Eisenberg, D., Schwarz, E., Komaromy, M., and Wall, R. (1984) *J. Mol. Biol. 179*, 125−142.

BI0101805